Rhythms Produced by High-Amplitude Periodic Stimulation of Spontaneously Beating Aggregates of Embryonic Chick Ventricular Myocytes[a]

MICHAEL R. GUEVARA[b] AND ALVIN SHRIER

Department of Physiology
McGill University
Montreal, Quebec,
Canada H3G 1Y6

INTRODUCTION

There have been many experiments carried out in which a variety of spontaneously beating cardiac preparations have been subjected to periodic stimulation with a train of current pulses. There have also been many numerical studies on the response of limit-cycle oscillators to periodic forcing. Theoretically, there are basically three classes of rhythms that can be observed when a limit-cycle oscillator is driven with a periodic input: (1) periodic rhythms, in which there is a phase locking of the oscillator to its input, with the input stimuli falling at well-defined phases of the oscillation; (2) quasi-periodic rhythms, which are nonperiodic rhythms in which there is a gradual progressive shift in the phase of the oscillation at which the stimulus falls; and (3) aperiodic rhythms, which are associated with chaotic dynamics.

In several instances, the response of a cardiac preparation to premature stimulation has been used to predict its response to periodic stimulation.[1-8] The effect of injecting a premature stimulus into a spontaneously beating preparation is to phase-reset the rhythm of oscillation. Winfree has stated that there are essentially two qualitatively different kinds of phase resetting in biological oscillators: type 1, which is seen at low amplitudes of stimulation, and type 0, which is seen at high amplitudes of stimulation.[9] We have previously shown in experiments on embryonic chick ventricular cells[10,11] and in numerical work on ionic models of Purkinje fiber[12] and the sinoatrial node[13] that, when type 1 resetting occurs, the new phase is a monotonically increasing function of the old phase, provided that the stimulus amplitude is sufficiently low. For higher stimulus amplitudes, the function becomes nonmonotonic, but the phase resetting remains type 1. For a sufficiently high amplitude of stimulation, type-1 phase resetting is no longer seen: it is replaced by type-0 phase resetting.[10-14] We describe below the behaviors seen in a simple model, and in experiments on heart cell aggregates, when periodic stimulation at such high amplitudes is applied. Both the modeling[15] and the experimental[10] work have been previously described.

[b]To whom correspondence should be addressed.

METHODS

Aggregates of ventricular cells are formed from a suspension of single cells dissociated from 7-day-old embryonic chick hearts, using methods earlier described.[11] At an external potassium concentration of 1.3 mM, these aggregates beat spontaneously at a relatively constant rate (see fig. 1 of reference 11). A microelectrode is introduced into one cell of the aggregate to record the transmembrane potential. The cells within an aggregate are very well coupled, so that the aggregate as a whole may be viewed as isopotential (see fig. 2 of reference 11). Periodic stimulation is applied by injecting a train of constant-current pulses through the same microelectrode used for recording the transmembrane potential.

MODELING RESULTS

FIGURE 1 shows a simple two-dimensional limit-cycle oscillator studied by several investigators over the years.[9,15-20] The state point of the system traverses the limit cycle (the circular path) at a constant velocity such that a complete cycle takes one time unit. One can paramaterize the limit cycle in terms of "phase," denoted by ϕ, with $\phi = 0$ being arbitrarily taken at the crossing of the positive x-axis by the limit-cycle trajectory. We perturb the oscillator with stimuli that are impulses of amplitude b. The effect of delivery of one such stimulus is to translate the state point at arbitrary phase ϕ by a distance b in a direction parallel to the positive x-axis (FIG. 1). We then assume that the state point instantaneously relaxes back to the limit cycle along a radial direction. Thus, the effect of delivering an isolated stimulus is to instantaneously "phase reset" the oscillator, producing a "new phase" of θ from the "old phase" of ϕ. One can write an equation

$$\theta = g(\phi, b), \tag{1}$$

using elementary trigonometry (eqs. (4) and (5) of reference 15). Thus, the new phase is a function only of the old phase and the amplitude of stimulation.

Let us now subject the oscillator to a periodic train of impulses, with τ being the time between delivery of individual impulses. One can then write

$$\phi_{i+1} = g(\phi_i, b) + \tau \qquad (\text{modulo } 1), \tag{2}$$

where ϕ_i is the phase of the oscillator immediately before the delivery of the ith impulse of the periodic stimulation train.[15] Equation 2 is a one-dimensional finite-difference equation, and is often called the Poincaré map. It can be iterated as follows: for any b and τ, given any starting value ϕ_1, compute ϕ_2 from equation 2; then, use equation 2 again with ϕ_2 inserted in its right-hand side to compute ϕ_3; and so on.

FIGURE 2 shows the results of iterating equation 2 for $b \geq 1.6$ in the range $0.0 \leq \tau \leq 1.0$. This range of b is at a rather high stimulus amplitude, being within the upper end of the type-0 region. For $b < 1$, type-1 phase resetting occurs. There are five different "phase-locking zones" present in FIGURE 2: 1:0, 2:0, 2:1, 2:2, and 1:1 zones. At any (τ, b) combination lying in the interior of a given $N{:}M$ phase-locking zone (N, M integers, $N \geq 1$, $M > 0$), an $N{:}M$ phase-locked rhythm will be seen. An $N{:}M$ phase-locked rhythm occurs when there is a repeating pattern of identical cycles, each
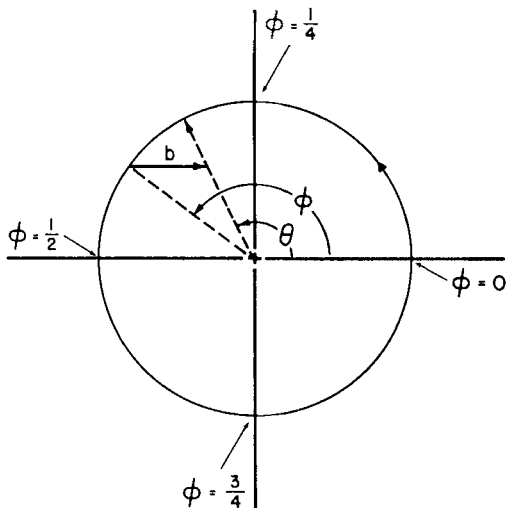
FIGURE 1. The circle with the arrow has unit radius and the trajectory proceeds in the direction indicated by the arrow. The effect of an isolated stimulus of amplitude b is to instantaneously reset the phase of the oscillator from an old phase ϕ to a new phase θ. (After fig. 1 of Guevara and Glass.[15] Reproduced by permission.)

consisting of N stimuli and M "events." The definition of an event is arbitrary:[10,12,13,21] we take a crossing of the positive x-axis by the limit-cycle trajectory (i.e., through $\phi = 0$) as our event marker. If one associates the x-axis in FIGURE 1 with transmembrane potential, this event would be associated with the peak or overshoot of the action potential, and the stimulus would be associated with an instantaneous depolarization of the membrane by a voltage independent of the phase of the cycle at which the stimulus is delivered. At all values of b in FIGURE 2, the 1:1 zone is encountered provided that τ is chosen sufficiently large, while the 1:0 zone is encountered for τ sufficiently small. As stimulation frequency is increased (i.e., τ decreased) for $b < 2.0$, the 1:1 zone is replaced by a 2:2 zone, in which 2:2 phase-locked rhythms can be seen. In a 2:2 rhythm,
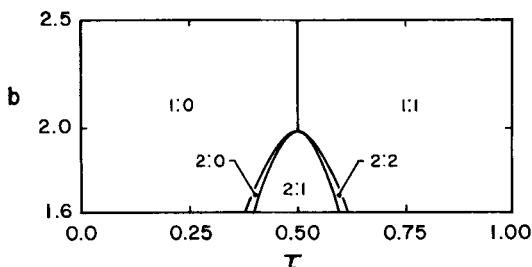
FIGURE 2. Phase-locking zones for $1.6 \leq b \leq 2.5$, $0.0 \leq \tau \leq 1.0$. Only five zones exist: 1:0, 2:0, 2:1, 2:2, and 1:1. (After fig. 2A of Guevara and Glass.[15] Reproduced by permission.)

while there is still an event produced by each stimulus, the phase in the cycle at which the stimulus falls alternates from stimulus to stimulus, with one phase occurring on even-numbered stimuli, and the other phase occurring on odd-numbered stimuli. As τ is decreased further, a 2:1 zone is encountered in which 2:1 phase-locked rhythms are found. In a 2:1 rhythm, the positive x-axis is crossed only once for every two stimuli delivered. Further decrease in τ leads to entry into a 2:0 zone. In the 2:0 rhythms met therein, the positive x-axis is never crossed by the trajectory, but alternate stimuli find the oscillator at the same phase. Eventually, for τ sufficiently small, a 1:0 zone containing 1:0 rhythms is produced. In a 1:0 rhythm, the trajectory never crosses the positive x-axis, but instead repeatedly traverses the same limited arc of the unperturbed limit cycle. Each stimulus, however, finds the oscillator at the same phase of its cycle.

For $b > 2.0$, the preceding situation is changed. As τ is decreased, there is a direct transition from a 1:1 to a 1:0 rhythm: the 2:2, 2:1, and 2:0 zones are no longer present (FIG. 2). For $b < 1.25$ (not shown), the behavior becomes increasingly complex, with chaotic and quasi-periodic dynamics being seen[15,17-19] (see Discussion).

FIGURE 2 was obtained by iterating equation 2 at many (τ, b) values in the (τ, b) parameter plane of FIGURE 2. One obtains little insight into FIGURE 2, however, from such purely arithmetical computations. The global organization of FIGURE 2 can be better appreciated if one graphically iterates equation 2 at a fixed (τ, b) point in FIGURE 2. We now do this at six different values of τ, keeping b fixed at 1.6.

FIGURE 3a shows the Poincaré map (i.e., equation 2) for $\tau = 0.75$. Note that the average slope of this map is zero, and that it has two extrema: this is a direct consequence of the fact that, for $b > 1.0$ in the model of FIGURE 1, type-0 phase resetting is occurring.[15,17] The result of iterating equation 2 graphically from an initial condition of $\phi_1 = 0.3$ is shown by the line with the arrow. Successive iterates converge to a period-1 orbit at a phase of about 0.64, corresponding to a 1:1 phase-locked rhythm with each stimulus coming in at a time about two-thirds of the way through the cycle. Note that the iterations shown in this example produce a transient due to the particular initial condition ($\phi_1 = 0.3$) chosen. If one were to choose a value of ϕ_1 exactly equal to the position of the period-1 point (i.e., $\phi_1 = 0.64$), no transient would be seen.

We now investigate the effect on the map of increasing the stimulation frequency (i.e., decreasing τ). From equation 2, it is obvious that decreasing τ has the effect of simply moving the map down by a fixed amount. FIGURE 3b shows the map for $\tau = 0.61$. If the map is iterated, and one examines the steady-state pattern after the transient due to initial conditions has dissipated, one sees that the stable period-1 orbit is no longer present, but is replaced by a period-2 orbit that alternates between two phases at about 0.51 and 0.59, producing a 2:2 phase-locked rhythm. This period-2 orbit comes about as a result of a period-doubling bifurcation, which occurs when the slope of the map at the period-1 point becomes more negative than -1.[15] The period is doubled, since two iterations are now required instead of one, to return back to the same state. While further decrease in τ to 0.60 preserves the period 2-orbit (FIG. 3c), this orbit now corresponds to a 2:1 rhythm, since one of the two phases on the orbit is now lying at 0.497, a value just less than 0.5. Injection of a stimulus at this phase takes the state point of the system to a phase on the limit cycle somewhere between 0 and 0.25, since $b > 1$ (see FIG. 1). Thus, a crossing of the positive x-axis is missed, and a 2:1 cycle results. Mathematically, this (2:2 → 2:1) transition is associated with a change in

the rotation number and is *not* due to a bifurcation, since the same period-2 orbit exists in both cases.[15] When $N:M$ phase locking exists, the rotation number is given by the ratio M/N. The 2:1 rhythm is preserved as τ is decreased (FIG. 3d) until a second change in rotation number occurs, leading to a 2:0 rhythm (FIG. 3e). The period-2 orbit in this case alternates between two values, both of which are less than 0.5; the positive x-axis is never crossed.

Finally, as τ is decreased further at this stimulus amplitude, the slope of the map at the period-1 point becomes less negative than -1, a period-halving or reverse period-
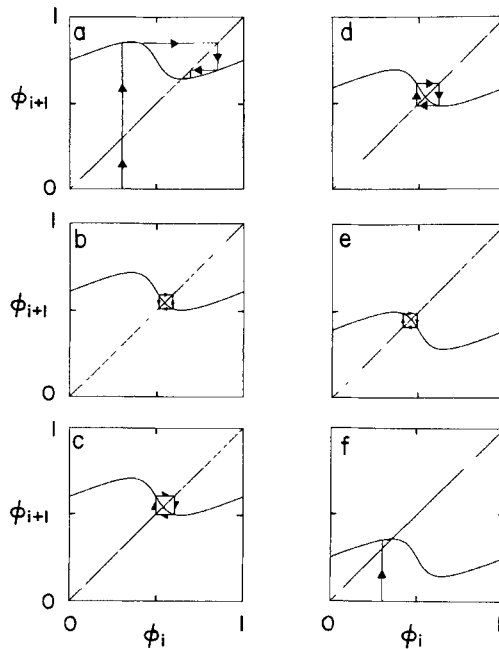
FIGURE 3. Poincaré maps resulting from the circle model of FIG. 1 with $b = 1.6$. The initial condition is $\phi_1 = 0.3$ in all cases. (**a**) $\tau = 0.75$: period-1 orbit: 1:1 phase locking. (**b**) $\tau = 0.61$: period-2 orbit: 2:2 phase locking. (**c**) $\tau = 0.60$: period-2 orbit: 2:1 phase locking. (**d**) $\tau = 0.59$: period-2 orbit: 2:1 phase locking. (**e**) $\tau = 0.39$: period-2 orbit: 2:0 phase locking. (**f**) $\tau = 0.25$: period-1 orbit: 1:0 phase locking. Transients are suppressed in (b)–(e). (After fig. 7-2 of Guevara.[10] Reproduced by permission.)

doubling bifurcation results, and the period-2 orbit disappears, being replaced by a stable period-1 orbit, corresponding to 1:0 phase locking (FIG. 3f).

The existence of the period-doubled phase-locking zones in FIGURE 2 (2:0, 2:1, 2:2) is a direct result of the period-doubling and period-halving bifurcations and changes in rotation number shown in FIGURE 3. These bifurcations in turn hinge upon the existence in the map of a region of negative slope where that slope is more negative than -1. For a stimulus amplitude $b > 2.0$, such a region does not exist in the map, and period-doubled orbits do not occur. There is thus a direct transition from a 1:1 to a 1:0

rhythm as τ is decreased for $b > 2.0$ (FIG. 2). This {1:1 → 1:0} transition is again not a bifurcation, being the result of a change in rotation number, in a manner similar to that producing the {2:2 → 2:1} and {2:1 → 2:0} transitions for $b < 2.0$.

EXPERIMENTAL RESULTS

The analysis of the simple—perhaps even simplistic—model of FIGURE 1 in terms of the Poincaré map (FIG. 3) suggests that similar behaviors should be found in a cardiac oscillator when the stimulus amplitude is high enough so as to produce type-0 phase resetting. We now demonstrate that this is in fact the case.

FIGURE 4 shows the effect of increasing the frequency of stimulation of an embryonic chick ventricular heart-cell aggregate with a train of 20-ms-duration depolarizing current pulses. At $t_s = 140$ ms (t_s is the time between stimuli), a 1:1 rhythm is seen, with each stimulus producing an action potential (FIG. 4a). As t_s is reduced to 130 ms, a 1:1 rhythm is eventually established, following a transient episode of marked alternans (FIG. 4b). At $t_s = 120$ ms, a maintained 2:2 or alternans rhythm is seen (FIG. 4c), in which there is a beat-to-beat alternation in action potential morphology. At $t_s = 110$ ms, a 2:1 rhythm occurs (FIG. 4d). Thus, the sequence of transitions seen as t_s is decreased is {1:1 → 2:2 → 2:1}, exactly as in the simple model (FIGS. 2 and 3a–c).

With further decrease in t_s, one might expect to see the sequence of transitions {2:1 → 2:0 → 1:0} as in the simple model of FIGURE 1. We have, however, only rarely seen this sequence in our experiments. We attribute this seeming rarity to technical problems. Since the cells in our aggregates are of embryonic origin and are therefore small (~10 μm diameter), and the aggregates beat vigorously, high-resistance micro-electrodes (typically, 40–60 MΩ) must be used in order to obtain long-lasting impale-ments. When attempting to pass high-amplitude currents (>20 nA) at high rates of stimulation ($t_s < 100$ ms), such electrodes often fail, in that the current delivered no longer remains constant from stimulus to stimulus. It is thus only on rare occasions that we have been able to obtain a train of constant-current pulses at high stimulation amplitude and frequency. The right part of FIGURE 5a shows a 2:0 rhythm, which developed out of what could be described as a 2:1 transient. Upon decrease of t_s by 5 ms to 50 ms (FIG. 5b), a 1:0 rhythm was seen following a 2:0 transient. The transient became monotonic when t_s was lowered still further to 40 ms (FIG. 5c).

Thus, the experimental work provides evidence for the transitions {1:1 → 2:2 → 2:1} and {2:1 → 2:0 → 1:0} seen in the simple model of FIGURE 1. Can one also then carry out an analysis similar to that shown in FIGURE 3, in which the phase-resetting response is used to construct a Poincaré map that can then be iterated? The filled circles in FIGURE 6a represent data points obtained from a phase-resetting experiment, and a curve is drawn through these points by hand. This curve is the new phase–old phase curve, equivalent to the function g in equation 1.

FIGURE 6a shows the result of iterating the map (equation 2, with $g(\phi, b)$ replaced by the experimentally determined new phase–old phase curve and τ replaced by t_s divided by the intrinsic beating interval of the aggregate) for $\tau = 1.0$, starting with $\phi_1 = 0.5$. The iterates converge to a period-1 orbit, corresponding to a 1:1 phase-locked rhythm. In a manner strictly analogous to that previously shown in FIGURE 3 for the
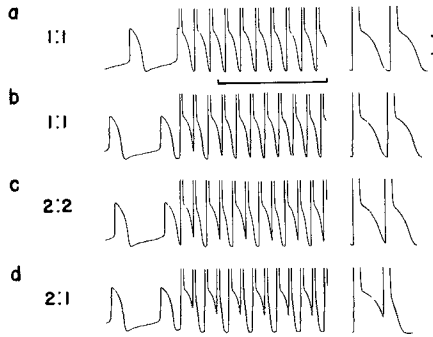
FIGURE 4. Transmembrane potential as a function of time. The traces on the left show the start of stimulation, while the traces on the right (at an expanded ($\times 2.5$) time scale) show the steady-state rhythm. (**a**) 1:1 phase-locking rhythm ($t_s = 140$ ms). (**b**) 1:1 phase-locking rhythm ($t_s = 130$ ms). Note the transient alternans at the start of stimulation. (**c**) 2:2 phase-locking rhythm ($t_s = 120$ ms). The trace at right shows that there is an alternation of action potential amplitude and duration in the steady state. A period-doubling bifurcation has taken place somewhere between $t_s = 130$ ms and $t_s = 120$ ms. (**d**) 2:1 phase-locking rhythm ($t_s = 110$ ms). Pulse amplitude = 40 nA. Pulse duration = 20 ms. Aggregate diameter = 114 μm. The off-scale vertical deflections are stimulus artefacts. *Vertical calibration bar:* 0 to -50 mV; *horizontal calibration bar:* 1 s. (After fig. 4-15 of Guevara.[10] Reproduced by permission.)

simple model, decrease of τ leads successively to 2:2 (FIG. 6b), 2:1 (FIG. 6c and d), 2:0 (FIG. 6e), and 1:0 (FIG. 6f) rhythms. Again, the {1:1 $\rightarrow$ 2:2} transition is due to a period-doubling bifurcation, the {2:0 $\rightarrow$ 1:0} transition to a period-halving bifurcation, and the {2:2 $\rightarrow$ 2:1} and {2:1 $\rightarrow$ 2:0} transitions to changes in rotation number. We stress that the value of t_s at which a change in rotation number occurs is arbitrary, in that it depends upon the particular definition of event marker chosen. A good
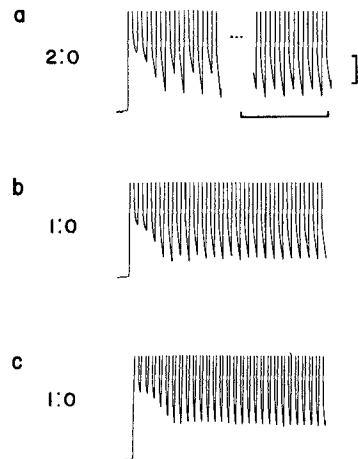
FIGURE 5. (**a**) 2:0 phase-locking rhythm ($t_s = 55$ ms). Upon prolonged stimulation, this 2:0 rhythm converted into a 1:0 rhythm. A 2:0 or 2:1 transient is seen initially. (**b**) 1:0 phase-locking rhythm ($t_s = 50$ ms). Note transient alternation at the beginning of the trace. (**c**) 1:0 phase-locking rhythm ($t_s = 40$ ms). Note the monotonic (i.e., not alternating) nature of the transient. Calibration bars as in FIGURE 4, except time bar is 0.5 s. Due to saturation in the current measurement circuitry, the current amplitude could not be determined in this experiment. However, it was greater than 50 nA. Pulse duration = 20 ms. Aggregate diameter = 160 μm. Different aggregate from that used in FIGURES 4 and 6. (After fig. 4-20 of Guevara.[10] Reproduced by permission.)
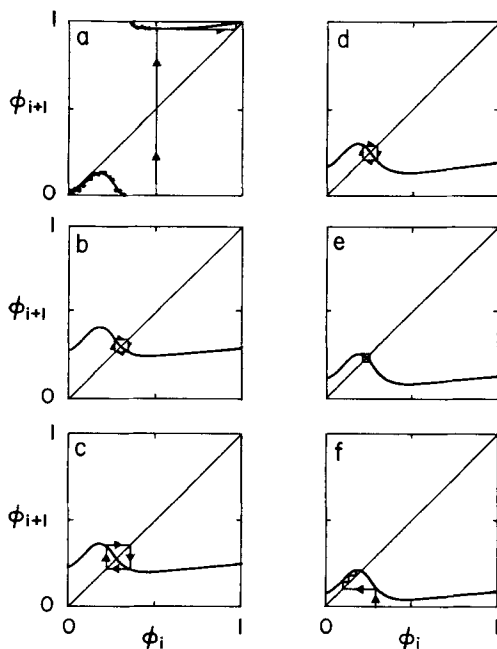
FIGURE 6. (a) $\tau = 1.00$: period-1 orbit, 1:1 rhythm. This Poincaré map is equivalent to the new phase–old phase curve, since $\tau = 1.00$ (see equation 2). The curve through the data points is hand-drawn. (b) $\tau \simeq 0.27$: period-2 orbit, 2:2 rhythm. (c) $\tau \simeq 0.22$: period-2 orbit, 2:1 rhythm. (d) $\tau \simeq 0.17$: period-2 orbit, 2:1 rhythm. (e) $\tau \simeq 0.12$: period-2 orbit, 2:0 rhythm. (f) $\tau \simeq 0.07$: period-1 orbit, 1:0 rhythm. $\phi_1 = 0.5$ (a), 0.3 (b–f). Phase-resetting data in (a) are taken from same aggregate as in FIGURE 4, for same pulse amplitude (40 nA) and pulse duration (20 ms). The second transient new phase[10,21] is plotted. The intrinsic interbeat interval during collection of these data was about 440 ms. The sequence of maps shown here also predicts the existence of the sequence of transitions {1:1 → 2:2 → 2:3 → 2:4 → 1:2} seen experimentally as t_s is raised to values larger than the intrinsic interbeat interval.[22] (After fig. 5-16 of Guevara.[10] Reproduced by permission.)

physiological example of this is the {2:2 → 2:1} (or {2:1 → 2:0}) transition, in which one has to have an (arbitrary) criterion of what is an action potential. For the iterations shown in FIGURE 6, the event marker is taken at $\phi = 0.25$, since one obtains action potentials for stimuli delivered at $\phi > 0.25$ during a phase-resetting experiment (see reference 10 for further explanation of this point). The agreement between the predictions of FIGURE 6 and the experiment of FIGURE 4 is quantitative, with, for example, the range of t_s over which the 2:2 rhythm is predicted to occur being on the order of 10 ms.

FIGURE 4b showed that there was an episode of transient alternans in the experiment before a maintained 1:1 rhythm was established. FIGURE 7 shows how this can be accounted for in terms of the Poincaré map, when the slope of the map at the stable period-1 orbit is negative. Transient alternation can also be seen experimentally in the approach to a 1:0 (FIG. 5b) rhythm, and is also accounted for by a region of negative

FIGURE 7. $\tau \simeq 0.36$: period-1 orbit, 1:1 phase locking. Iteration predicts that a phase of transient alternans should be seen before asymptotic establishment of a 1:1 rhythm. Poincaré map formulated from same phase-resetting data as in FIGURE 6. (After fig. 5-17 of Guevara.[10] Reproduced by permission.)
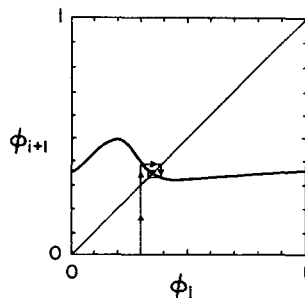
slope in the vicinity of the period-1 orbit on the Poincaré map. In the experimental work, the approach to a maintained 2:2 rhythm is often alternating, with a gradual progressive decrease in the degree of alternans often being seen (FIG. 4c); once again, this alternating approach is due to a negative-slope region of the Poincaré map. Should τ be increased enough in FIGURE 7 so that the period-1 orbit lies at $\phi > 0.45$, that orbit would lie on a region of positive slope in the map and a monotone, not an alternating, approach to the steady state, would be seen (FIG. 3a shows the equivalent case in the simple model). This monotonic approach fits with the experimental findings at sufficiently high values of τ. Similar reasoning (FIG. 6f) explains why a monotonic transient is seen experimentally in the run-up to the 1:0 rhythm at sufficiently small t_s (FIG. 5c).

DISCUSSION

Discrepancies between Simple Model and Experiment

There are striking similarities between the response to high-amplitude periodic stimulation of the simple model of FIGURE 1 and the aggregate. These similarities are essentially traceable to the fact that the new phase–old phase curves of the two systems are quite similar (FIGS. 3 and 6). We now draw attention to three discrepancies between the two systems:

(1) In the simple model of FIGURE 1, one finds only two rhythms at the highest amplitudes of stimulation, 1:1 and 1:0 (FIG. 2). We have not seen this in our experiments in aggregates, probably because we have not been able to pass sufficiently high currents through the microelectrode. Such a transition can be seen in isolated single rabbit ventricular myocytes, however, where use of a rather large bore suction electrode allows relatively large currents (in terms of microamperes per square centimeter) to be passed (Guevara and Jeandupeux, unpublished).

(2) The new phase–old phase curve in the simple model is symmetric (FIG. 3), while it is not so in the experiments (FIG. 6). The symmetry in the former case leads to symmetric phase-locking zones (FIG. 2), which is not the case in experiment (fig. 9 of reference 22).

(3) Due to the infinitely fast relaxation of the trajectory back to the limit cycle following delivery of a stimulus, the first transient new phase–old phase curve[10,12,13,21]

can be iterated in the simple model. In contrast, at high stimulus amplitudes in the experimental work, when graded action potentials are produced, the relaxation back to the limit cycle takes longer than one cycle, and the second transient new phase–old phase curve, which is an excellent approximation to the asymptotic new phase–old phase curve,[10] must be used (as in FIG. 6).

Rhythms Seen at Lower Stimulus Amplitudes

In the simple model, we have presented results for $b > 1.6$. As b is decreased to below about 1.25, there is a cascade of period-doubling bifurcations leading to period-4, 8, 16, ... orbits, culminating in chaotic dynamics.[15,18,19] The Poincaré maps generating these higher order period-doubling bifurcations are similar to those shown in FIGURE 3, but have a steeper slope. Similar behavior has been described in other degree-0 maps.[23–25] As b is decreased to below 1.0, there is a discontinuous transition from a degree-0 map to a degree-1 (invertible) map. In the latter case, there is the usual Arnol'd-tongue structure of phase-locking zones, with a periodic–quasi-periodic sequence of rotation number;[5,15,26] chaos does not exist. In contrast, in the aggregates, as stimulus amplitude is reduced, there is a transition from a degree-0 map to a discontinuous map, then to a degree-1 (noninvertible) map, and finally to a degree-1 (invertible) map.[10] The traces shown in FIGURES 4 and 5 are at current amplitudes toward the upper end of the type-0 region. We have not systematically studied the response of the aggregate to stimulation at the lower amplitude end of the type-0 region, where one might expect period-doubling cascades to chaotic dynamics, as in the simple model. The transition $\{2{:}1 \rightarrow 4{:}2\}$ seen in the simple model at the bottom end of the type-0 region ($1.25 < b < 1.00$), however, has been seen in experiments on aggregates.[22] This 4:2 rhythm is a period doubling of the 2:1 rhythm, and thus arises out of the 1:1 rhythm via two successive period-doubling bifurcations. The transition from a 4:2 rhythm to chaotic dynamics seen in the model as τ is reduced has not been described in the aggregate, due to our inability to maintain the current pulse amplitude constant at the high rate and amplitude of stimulation needed. Chaotic dynamics can, however, be seen if the stimulus amplitude is reduced further so that a degree-1 (noninvertible) map is produced.[3] This form of chaotic dynamics is encountered when the aggregate is stimulated at a rate *lower* than its spontaneous rate. We have also not confirmed the existence of chaotic dynamics predicted to occur at stimulation rates *higher* than the intrinsic rate when the map is degree-1 (noninvertible). Finally, if the current amplitude is reduced to a low enough value, an Arnol'd-tongue structure similar to that seen in the simple model results in the experiments.[8]

In summary, in both model and experiment, at very low levels of stimulus amplitude, where type-1 (invertible) resetting is seen, there is a complex periodic–quasi-periodic sequence of rhythms that is well understood theoretically.[5] At intermediate levels, chaotic dynamics and bistability[3,5,17–19,22] (two different rhythms at the same set of stimulation parameters) can be seen. At very high levels (i.e., at the top end of the type-0 range), a simple sequence containing relatively few rhythms is seen (FIGS. 2 and 6). This reduction in the number of possible rhythms, and the disappearance of complex behaviors, such as chaotic dynamics and bistability, is seen in many simple limit-cycle oscillators as stimulus amplitude is increased.[16,19,27–30]

Connection with Quiescent Systems

A glance at the traces in FIGURES 4 and 5 clearly demonstrates that the behaviors shown there do not hinge upon the existence of spontaneous activity in the preparation. It is quite evident that the existence or nonexistence of spontaneous diastolic depolarization plays little or no role in the generation of these rhythms. In fact, the transition $\{1:1 \rightarrow 2:2 \rightarrow 2:1\}$ has been described in quiescent aggregates,[31] in isolated rabbit ventricular myocytes,[32] and in the Beeler–Reuter model of quiescent ventricular muscle.[32] In addition, the transition $\{1:1 \rightarrow 2:2 \rightarrow 2:1 \rightarrow 4:2 \rightarrow chaos\}$ has been seen in isolated rabbit ventricular cells (Guevara, Jeandupeux, and Alonso, unpublished) and in the corresponding ionic modeling work (Lewis and Guevara, unpublished). The analysis of the response of quiescent preparations involves consideration, not of phase as in the case of spontaneously active preparations, but of action potential duration, and results in discontinuous maps containing two or more monotonically decreasing branches. While such maps can also display period-doubling bifurcations and bistability, it remains to be seen how their bifurcation structure, which has not been studied in detail, differs from that of degree-0 circle maps such as those presented in FIGURES 3 and 6.

Implications for Ventricular Arrhythmias

During coronary occlusion, the phase of induction of ventricular arrhythmias such as tachycardia and fibrillation is often immediately preceded by a phase of electrical or mechanical alternans (see reference 10 for references). There is also one recently published report that shows clear evidence of a period-4 rhythm during ischaemia (fig. 2C of reference 33). For b lying between about 1.0 and 1.2 in the simple model, chaotic dynamics exists, associated with period-doubling bifurcations. In light of the correspondences previously drawn between the response of spontaneously active and quiescent systems, and between degree-0 circle maps and two-branched interval maps, it is tempting to speculate that, as ischaemia becomes more profound, the operating point of cells in the ventricle is effectively moving downwards in a parameter plane equivalent to the (τ, b) plane of FIGURE 2, due to a decrease both in the excitability of the cells and in the size of the excitation current.[10] This would eventually result in two successive period-doubling bifurcations corresponding to alternans and period-4 (4:2, 4:4) rhythms, which might then progress on to chaotic dynamics,[34] initiating ventricular fibrillation.

REFERENCES

1. MOE, G. K., J. JALIFE, W. J. MUELLER & B. MOE. 1977. Circulation **56**: 968–979.
2. SCOTT, S. W. 1979. Stimulation simulations of young yet cultured beating hearts. Ph.D. thesis. State University of New York (Buffalo), Buffalo, N.Y.

3. GUEVARA, M. R., L. GLASS & A. SHRIER. 1981. Science **214:** 1350–1353.
4. YPEY, D. L., W. P. M. VAN MEERWIJK & R. L. DEHAAN. 1982. *In* Cardiac Rate and Rhythm, L. N. Bouman and H. J. Jongsma, Eds.: 363–395. Martinus Nijhoff. The Hague, The Netherlands.
5. GLASS, L., M. R. GUEVARA, J. BELAIR & A. SHRIER. 1984. Phys. Rev. **29A:** 1348–1357.
6. GLASS, L., M. R. GUEVARA & A. SHRIER. 1987. Ann. N.Y. Acad. Sci. **504:** 168–178.
7. SHRIER, A., H. DUBARSKY, M. ROSENGARTEN, M. R. GUEVARA, S. NATTEL & L. GLASS. 1987. Circulation **76:** 1196–1205.
8. GUEVARA, M. R., A. SHRIER & L. GLASS. 1988. Am. J. Physiol. **254:** H1–H10.
9. WINFREE, A. T. 1980. The Geometry of Biological Time. Springer-Verlag. New York/ Berlin.
10. GUEVARA, M. R. 1984. Chaotic cardiac dynamics. Ph.D. thesis. McGill University. Montreal, P.Q., Canada.
11. GUEVARA, M. R., A. SHRIER & L. GLASS. 1986. Am. J. Physiol. **251:** H1298–H1305.
12. GUEVARA, M. R. & A. SHRIER. 1987. Biophys. J. **52:** 165–175.
13. GUEVARA, M. R. & H. J. JONGSMA. 1990. Am. J. Physiol. In press.
14. VAN MEERWIJK, W. P. M., G. DEBRUIN, A. C. G. VAN GINNEKEN, J. VAN HARTEVELT, H. J. JONGSMA, E. W. KRUYT, S. S. SCOTT & D. L. YPEY. 1984. J. Gen. Physiol. **83:** 613–629.
15. GUEVARA, M. R., & L. GLASS. 1982. J. Math. Biol. **14:** 1–23.
16. MINORSKY, N. 1962. Nonlinear Oscillations. Van Nostrand. Princeton, N.J.
17. HOPPENSTEADT, F. C. & J. P. KEENER. 1982. J. Math. Biol. **15:** 339–346.
18. KEENER, J. & L. GLASS. 1984. J. Math. Biol. **21:** 175–190.
19. DING, E. J. 1988. Phys. Scr. **38:** 9–16.
20. SCHAMROTH, L., D. H. MARTIN & M. PACHTER. 1988. Am. Heart J. **115:** 1363–1368.
21. KAWATO, M. 1981. J. Math. Biol. **12:** 13–30.
22. GUEVARA, M. R., A. SHRIER & L. GLASS. 1990. *In* Cardiac Electrophysiology: From Cell to Bedside, D. P. Zipes and J. Jalife, Eds. Saunders. Philadelphia. In press.
23. HOPF, F. A., D. L. KAPLAN, H. M. GIBBS & R. L. SHOEMAKER. 1982. Phys. Rev. **25A:** 2172–2182.
24. MANDEL, P. & R. KAPRAL. 1983. Opt. Commun. **47:** 151–156.
25. BELAIR, J. & L. GLASS. 1985. Physica **15D:** 143–154.
26. GLASS, L., A. SHRIER & J. BELAIR. 1986. *In* Chaos, A. V. Holden, Ed.: 237–256. Manchester University Press. Manchester, England.
27. HAYASHI, C., H. SHIBAYAMA & Y. NISHIKAWA. 1960. IRE Trans. Circ. Theory **CT-7:** 413–422.
28. FLAHERTY, J. B. & F. C. HOPPENSTEADT. 1978. Stud. Appl. Math. **58:** 5–15.
29. TOMITA, K. & T. KAI. 1979. J. Stat. Phys. **21:** 65–86.
30. GONZALES, D. L. & O. PIRO. 1983. Phys. Rev. Lett. **50:** 870–872.
31. GUEVARA, M. R., G. WARD, A. SHRIER & L. GLASS. 1984. *In* Computers in Cardiology: 167–170. IEEE Comp. Soc. Silver Spring, Md.
32. GUEVARA, M. R., F. ALONSO, D. JEANDUPEUX & A. C. G. VAN GINNEKEN. 1989. *In* Cell to Cell Signalling: From Experiments to Theoretical Models, A. Goldbeter, Ed.: 551–563. Academic Press. London.
33. DILLY, S. G. & M. J. LAB. 1988. J. Physiol. (London) **402:** 315–333.
34. SMITH, J. M. & R. J. COHEN. 1984. Proc. Natl. Acad. Sci. U.S.A. **81:** 233–237.